

# Polarizers for Extreme Ultraviolet Light

Brian Schwartz, University of Colorado, Physics 7810: Soft X-Ray Optics, spring 2001.

Polarized light is important is a valuable tool in discovering and exploiting material symmetries. At visible and near IR wavelengths, for example, polarized light reveals anisotropies in crystals. These crystals are now used as modulators to encode information onto optical carriers in the telecommunications industry.

Photons with energies in the EUV ( $\sim 30$ – $250$  eV,  $\lambda \approx 5$ – $40$  nm) and soft x-ray ( $\sim 250$ – $2.5$  keV,  $\lambda \approx 0.5$ – $5$  nm) regions have enough energy to ionize core atomic electrons. Hence, polarized light in this spectral region can reveal symmetry properties of atoms (Attwood, 1999). For example, polarization dependent x-ray absorption near electron ionization energies reveal an anisotropic charge distribution caused by either non-cubic point-group symmetries or magnetism (Collins, 1997).

Linearly polarizing optical components are made of materials that are either dichroic, birefringent, or have polarization sensitive reflectivity. In this work I will discuss polarizing components based on these mechanisms and their applicability to XUV light based on the following criteria:

1. polarization quality, measured by extinction ratio  $\frac{T_p}{T_s}$  or degree of polarization  $\frac{T_p - T_s}{T_p + T_s}$  ;
2. attenuation of polarized output;
3. spectral bandwidth;
4. effect of direction of incident beam.

## Dichroic Linear Polarizers

Linearly dichroic polarizing materials absorb light of one linear polarization state while absorbing light polarized orthogonal to the transmitted plane of polarization. The Polaroid H-Sheet, the most common dichroic polarizer, is a stretched sheet of polyvinyl alcohol impregnated with iodine atoms. Because the molecules are stretched in one direction, they have different absorptive properties for light polarized parallel and perpendicular to the stretch. Mathematically, this phenomenon translates into linear dichroism: an anisotropy in the imaginary part of the dielectric constant.

The transmission of a typical linearly dichroic polarizer, oriented with its pass axis parallel to the plane of incident light polarization, is only 50% and 500 nm, with an extinction coefficient of only 3:1. The performance further degrades at lower wavelengths.<sup>1</sup>

The Polaroid dichroic polarizer polarizes by the same mechanism as a wire grid polarizer, i.e., a planar structure composed of series of parallel conducting wires or strips. When the sheet of stretched vinyl molecule chains is dipped into an iodine-rich solution, the iodine accumulates along the vinyl chains, and its conduction electrons can move along the chains as if they were wires.

Consider unpolarized light incident on a vertical grid of thin conducting wires. The electric field components of the light parallel to the wires will drive conduction electrons in the wires and create a current. Because the wires are thin, we will consider current in the vertical direction only.

The impedance of the wires will cause the electrons to transfer some energy to the metal as heat. The accelerated electrons will also lose energy by reradiating light, which, in this case, is vertically polarized. The component of this light traveling in the direction of the incident light will incoherently interfere with the incident light and hence destructively interfere with any transmitted vertically polarized light. Now consider light polarized perpendicular to the wires. The electrons relatively immobile in this direction, so they absorb little horizontally polarized light. Hence, the wire grid acts like a polarizer that transmits light polarized normal to the wires (Hecht, 1998).

Bennett and Bennett (1978) summarize the transmission line models of Marcuvitz (1951) and Auton (1967) used to predict performance of wire grid polarizers. Auton showed that the widest spectral bandwidth occurs when the width of the metal strips,  $a$ , equals  $d$ , the spacing between their centers. In this case, the expressions for the transmitted polarization components are

---

<sup>1</sup> The Polaroid H-Sheet does polarize 33.17 keV ( $\lambda=0.037$  nm) x-rays ( $\frac{T_p}{T_s} = 1.22$ ,  $T_p = 27\%$ ), as such x-rays polarized along the polymer chains ionize iodine's K-shell electrons (Collins, 1997). Clearly the stretched material structure is an important factor in this phenomenon.

$$T_p = \frac{4nA^2}{1+(1+n)^2 A^2} \quad \text{and} \quad T_s = \frac{4nB^2}{1+(1+n)^2 B^2}, \quad \text{where}$$

$$B = \frac{d}{\lambda} \left[ 0.3466 + \frac{0.25Q_2}{1+0.25Q_2} + 0.003906 \left( \frac{d}{\lambda} \right)^2 \right], \quad A = \frac{1}{4B}, \quad (1.1-1)$$

$$\text{and } Q_2 = \frac{1}{\left[ 1 - \left( \frac{d}{\lambda} \right)^2 \right]^{\frac{1}{2}}} - 1.$$

Here,  $p$ -polarization is perpendicular to the grid wires, and  $s$ -polarization is parallel to them. As shown in Figure 1, these equations predict that a wire grid of period  $d$  will effectively polarize light of wavelength  $\lambda$  if  $d < \lambda/2$ . The grid severely attenuates smaller wavelengths and the extinction ratio  $\frac{T_p}{T_s}$  is approaches unity.

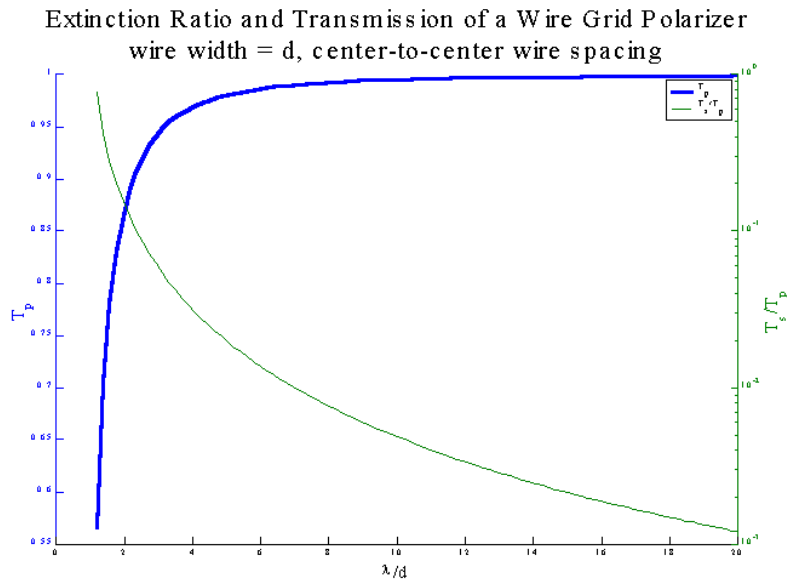


Figure 1: For effective polarization, the grid spacing of a wire grid polarizer must be less than the one-half wavelength of incident light.

Murnane and Kapteyn (1993) explain the significance of the  $\lambda/2$  grid spacing by considering the grid as set of parallel waveguides. For  $s$ -polarized light incident normal to the plane of the waveguides, the tangential component of the electric field is continuous across the air-metal boundary. Since gold is a good conductor, it holds no field, and the field in the waveguide is zero at the air-metal interface (or vacuum-metal for EUV or soft x-rays). The sinusoidal mode solutions in each waveguide limit  $m$ , the number of

allowed modes, to  $m < 2d/\lambda$ . For  $d < \lambda/2$ ,  $m = 0$ , and the grating structure does not guide  $s$ -polarized light through it.

The boundary conditions for  $p$ -polarized light are different from the  $s$ -polarized light. Since the electric field is normal to the air-metal interface, we must consider the normal component of the electric displacement  $\vec{D}$ . The conductivity of gold is nearly infinite, so the electric displacement is zero in the conductor, but a surface charge at the boundary creates a discontinuity in  $\vec{D}$  (Reitz, Milford, and Christy, 1993). Since different boundary conditions apply to the  $p$ -polarized light, same  $s$ -polarization mode cutoff does not apply. The surface charge allows the shape of the sinusoidal  $p$ -polarized (TM) mode to be wider than the  $s$ -polarized TE mode, so perhaps this makes the effective waveguide width larger, and hence allows for more modes.

G.R. Bird and M. Parrish, Jr. (1960) were among the first to demonstrate a wire grid polarizer. They fabricated such a polarizer for use in the near-IR (1.5 – 10  $\mu\text{m}$ ). They evaporated gold, or in some cases aluminum, onto a diffraction grating substrate such that the atoms accumulated in the grooves to create thin wires. Their width and spacing dimensions were less than a wavelength.

Since the work of Bird and Parrish, advances in photolithography has allowed for the manufacture of structures of increasingly small feature sizes. Tomada, *et al* (1997) used scanning electron micrography to make an aluminum wire-grid polarizer with a period of  $d = 0.36 \mu\text{m}$ . The wire widths ranged from  $\sim 0.40d$  to  $0.65d$ . They created a high transmittance ( $T_s = 80\%$ ,  $T_s / T_p = 30$ ) and by increasing the aluminum thickness from 156 nm to 286 nm, a high-extinction-ratio polarizer ( $T_s = 54\%$ ,  $T_s / T_p = 1000$ ) at  $\lambda = 780 \text{ nm}$ . Using the coupled mode theory of Gaylord and Moharam (e.g., 1987), Tomada, *et al* predicted a 150 nm spectral bandwidth for the high-transmittance polarizer, and a 100 nm bandwidth for the high extinction ratio polarizer.

For a wire-grid polarizer to work in the EUV ( $\lambda = 5\text{-}40 \text{ nm}$ ), the model of Auton and Marcuvitz, as described above, predict that grid period should not exceed  $\sim \lambda/2$ , or  $\sim 20 \text{ nm}$ . Results of Gruntman (1995) illustrate this requirement. He measured the transmission of unpolarized  $\lambda = 58.4 \text{ nm}$  light by a commercially available  $5 \times 11 \text{ mm}$  gold grating with a period  $d = 200 \text{ nm}$  and bar thickness  $a = 100 \text{ nm}$ . This

grating has a modest extinction ratio, 100:1, but the transmission  $T_p$  was just 2% at this wavelength, and decreased by an order of magnitude at  $\lambda=100$  nm.

Gruntman notes that fabrication technology limited the grating thickness, which was supported by a “large-mesh grid.” It’s possible that the 435 nm grating thickness caused much of the loss. At EUV wavelengths, the imaginary part of the refractive index,  $\beta$  takes on values between 0.001 ( $\lambda=5$  nm) and 0.55 ( $\lambda=41$  nm). The imaginary part of the refractive index contributes to an exponential decay in the electric field of  $e^{-\text{Im}(n)kz} = e^{-\frac{2\pi\beta}{\lambda}z}$ . The average intensity  $\bar{I}$  is then proportional to  $e^{-\frac{2\pi\beta}{\lambda}z}$ . The decay length is then  $l_{\text{abs}} = \frac{\lambda}{4\pi\beta}$ , which, for gold at  $\lambda=41$  nm, is just 6 nm (Attwood, 1999).

Kuta and Driel (1995) discussed the effect of grating thickness in their coupled wave analysis of metallic gratings. In agreement with the results of Tomada, *et al*, they predict both lower transmission and greater extinction coefficients as grating thickness increases. They attribute the two effects to, for *s*-polarization, lowered forward diffraction efficiency via absorption by the metal, and for *p*-polarization, exchange in energy between forward and backward diffracted waves as grating thickness changes.

Current advances in lithography suggest a better future for wire grid polarizers in the EUV. In 1995, Mitsubishi used x-ray lithography to make a memory chip with 140 nm feature sizes (Attwood, 1999). Progress since then includes Schattenburg *et al* (1997), who made a grating with a 100 nm period using interferences fringes. Researchers at Sandia National Labs have continued the development of EUV scale structures: They developed a 13 nm laser based on ionizing xenon gas clusters with a laser pulse. This source can produce 30 nm feature sizes, however with low yield (Hardin, 1999).

## Birefringent Polarizers

While dichroic materials are anisotropic in the imaginary part of the refractive index, birefringent materials are anisotropic in the real part. Most polarizers made of such materials, e.g., calcite and quartz, are uniaxial, that is, light polarized along the so-called crystal axis experiences an extraordinary refractive index,  $n_e$ , while linear polarized light oriented in all other directions experiences  $n_o$ , the ordinary index of refraction. Hence, light of any polarization propagating along the crystal axis of a uniaxial crystal experiences the same refractive index.

Birefringent polarizers consist of two right-angle prisms cemented together along the hypotenuse such that their respective crystal axes are orthogonal. The electric field of light incident normal to the first prism decomposes into its ordinary and extraordinary components: part of the light experiences  $n_o$ , and part of it experiences  $n_e$ . At the 45° interface with the second prism, the two components refract at different angles according to the Snell's Law and the refractive index each component experiences. An example is shown in Figure 2.

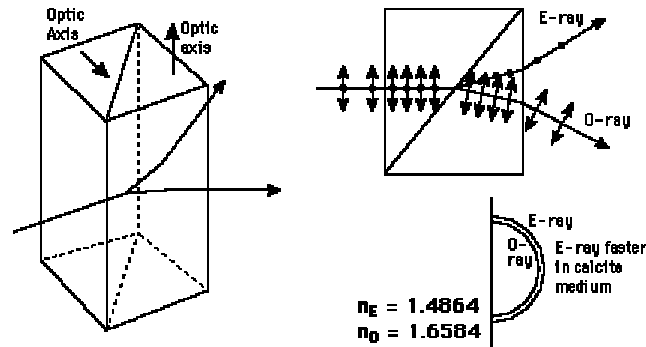


**Figure 2:** A Wollaston Prism, above, consists of two prisms made uniaxial materials bonded such that their crystal axis are orthogonal to each other. Ordinary polarization is in a plane normal to the optic axis, while extraordinary polarization is in a plane parallel to the optic axis (Knave, 2000).

For XUV and soft x-ray radiation, refractive indices are very close to 1, and are expressed as  $n = 1 - \delta + i\beta$ . As shown in Table 1, the refractive index of quartz and calcite differ by one part in a thousand at XUV wavelengths. I could not find any birefringence data at these wavelengths. Yet, it is instructive to calculate the birefringence at 10 nm assuming the ratio of birefringence to the deviation from vacuum index is independent of wavelength. As shown in Table 1, these values are 0.018 and 0.296 for quartz and calcite respectively.

**Table 1:** Birefringence of Quartz and Calcite at VIS and EUV wavelengths

	$n, \lambda = 589 \text{ nm}$ (Hecht, 1998)	$\frac{(n_e - n_o)}{n_{\text{avg}} - n_{\text{vac}}}$	$n, \lambda = 10 \text{ nm}$ (Gullikson, 2001)	$n_e - n_o$ (estimated)	$\beta, \lambda = 10 \text{ nm}$
quartz ( $\text{SiO}_2$ )	$n_o = 1.54$ $n_e = 1.55$	0.018	0.987	0.00023	0.013
calcite ( $\text{CaCO}_3$ )	$n_o = 1.66$ $n_e = 1.49$	0.296	0.988	0.0036	0.002

To find out how effective a Wollaston polarizer will be in for EUV light, we should find the angle between the ordinary,  $|o\rangle$ , and extraordinary,  $|e\rangle$ , beams exiting the second prism. As shown in Figure 2 and Figure 3,  $|o\rangle$  and  $|e\rangle$  are collinear in the first prism, as they enter it at normal incidence. At the interface, phase continuity requires the component of the wave vector tangent to the interface be conserved, so the ordinary ray in the first prism couples into the extraordinary mode in the second prism, and visa versa. This is shown in Figure 3.

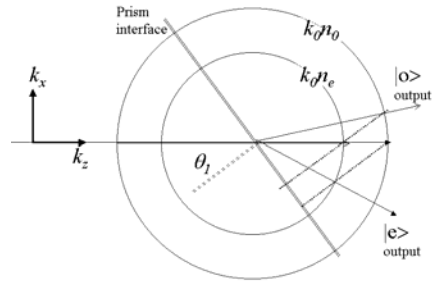


**Figure 3:** k-space diagram showing refraction in a Wollaston prism polarizer.

From Figure 3 we see the Snell's Law relations, with angles defined with respect to the interface normal, are

$$n_o \sin \theta_1 = n_e \sin \theta_{2e} \quad n_e \sin \theta_1 = n_o \sin \theta_{2o} \quad (2.1-1)$$

To find the angle between the ordinary and extraordinary beams at the prism output, we must reference the angles to the interface between the prism and the next medium (medium 3, usually vacuum):

$$\phi_{2e} = \theta_1 - \theta_{2e} \quad \phi_{2o} = \theta_1 - \theta_{2o} \quad (2.1-2)$$

Such that

$$n_e \sin \phi_{2e} = n_3 \sin \phi_{3e} \quad \text{and} \quad n_o \sin \phi_{2o} = n_3 \sin \phi_{3o} .$$

Using the above two equations, we can solve for the angle between the two exit beams:

$$\Delta = \phi_{3e} - \phi_{3o} .$$

For calcite at  $\lambda=589$  nm and  $\theta_1=45^\circ$ ,  $\Delta=14.6^\circ$ . For calcite at  $\lambda=10$  nm and  $\theta_1=45^\circ$ ,  $\Delta=0.2^\circ$ . If the input beams are 3 mm wide, the output ordinary and extraordinary beams will separate at a distance of 86 cm

past the polarizer output. This distance requirement is quite inconvenient, especially since soft x-ray and EUV optics are usually done in vacuum because of the absorbance of air.

If the reader still fancies using a calcite polarizer for soft x-rays or the EUV, a discussion of loss in calcite should change his mind. Recall the  $\frac{1}{e}$  intensity decay length,  $l_{abs} = \frac{\lambda}{4\pi\beta}$ . For calcite at  $\lambda=10$  nm, is just 40 nm. This decay length is so small that it makes the above angle considerations appear somewhat irrelevant.

## Brewster's Angle Polarizers

Given the difficulties of making dichroic and birefringent polarizers for UEV and soft x-ray regions discussed above, it is understandable the most common polarizers for this spectral range are based on Brewster's angle reflections of a material rather than transmission through a material. At Brewster's angle, the angle of refraction is the complement of the incident angle, that is,

$$\theta_2 = \frac{\pi}{2} - \theta_1, \quad (3.1)$$

or by Snell's Law,

$$\theta_1 = \theta_B = \arctan \frac{n_2}{n_1} \quad (3.2)$$

When this occurs, the  $p$ -polarized (in the plane of incidence) of the refracted light's electric field is parallel with the reflected light. Since light is a transverse wave, the reflected light contains no  $p$ -polarized components, and the reflected light is purely  $s$ -polarized. For EUV and soft x-ray light,  $n \approx 1$  for most materials, so  $\theta_2 \approx \theta_1$ , and by Eq. (3.1), Brewster's angle is  $\theta_B \approx \frac{\pi}{4}$ .

While using a Brewster's angle reflection polarizes the light to a high purity, the magnitude of the reflected light is small because of the small index differences between vacuum and materials at XUV wavelengths. Evaluating the Fresnel reflection coefficient for  $s$ -polarized light incident on fused silica ( $\text{SiO}_2$ ), a common mirror substrate, at Brewster's angle yields a reflectivity of

$$R_s = |r_s|^2 = \left| \frac{n_1 \cos \theta_1 - n_2 \cos \theta_2}{n_1 \cos \theta_1 + n_2 \cos \theta_2} \right|^2 = \left| \frac{1 - (1 - \delta + i\beta)^2}{1 + (1 - \delta + i\beta)^2} \right|^2 = 1.8 \times 10^{-4}. \quad (3.3)$$

This is quite a low value, and any optical component with such a loss is impractical.

To use the polarization purity of Brewster angle reflection without high losses, scientists have designed multilayer XUV and soft-ray mirrors optimized for reflection at Brewster's angle ( $\approx 45^\circ$ ). Dhez (1987) describes an Hf/Si multilayer coating with a reflectivity  $R_s > 25\%$  and a maximum degree of polarization  $P = \left| \frac{R_s - R_p}{R_s + R_p} \right|$  of 88% ( $\frac{R_s}{R_p} = 16$ ) at  $\lambda = 30.4$  nm. This design had a good input angle tolerance, as  $P > 80\%$  over a  $20^\circ$  range of incident angles centered around  $47^\circ$ .

Narrow spectral bandwidth is one drawback of such a polarizer, reports Maehara *et al* (1991). To use the multilayer polarizer at wavelengths other than the design wavelength, they need to be tilted to maximize polarization purity and throughput. This makes sense, as material dispersion changes Brewster's angle. Tilting the polarizer to maximize polarization purity is clearly inconvenient, as it requires one to realign the optical system whenever the wavelength changes.

To remove this problem while keeping the benefits of the multilayer polarizer, Maehara *et al* designed a double-multilayer polarizer (DMP). It consists of identical multilayer polarizers that are simultaneously rotated and translated such that the incident angles on the polarizers are optimized while the output beam remains stationary. With a pair of Ru/Si mirrors, they built a DMP with a degree of polarization exceeding 90% ( $\frac{R_s}{R_p} = 19$ ) between 80 and 120 eV (10-15 nm). Loss was still a problem, as reflectivity of unpolarized light ranged from 5 to 30 %.

Using a laterally graded multilayer mirror is a simpler way to increase spectral bandwidth (Attwood, 1999). Such a coating consists of layers of tapered thickness; so reflecting polarizer design wavelength is a function of location of the incident beam on the polarizer clear aperture. Hence one select a wavelength for optimum polarization by moving the polarizer with a translation stage that moves in the plane of the reflecting surface.

## Summary

In this work I have described polarizers based on dichroism, birefringence, and reflectivity. Table 2 summarizes the performance of the EUV polarizers discussed in this paper.

**Table 2:** Summary of EUV Polarizer Performance

Polarizer type	$\lambda$ , nm (theory)	Extinction ratio	Transmission, %	Change beam direction?	Reference
Wire grid 200 nm period	780 (700-850)	30	80	No	Tamada, et al, 1997
Wire grid 200 nm period	780 (750-850)	1000	54	No	Tamada, et al, 1997
Wire grid 200 nm period	58.4	100:1	2	No	Gruntman, 1995
Birefringent Prism, Calcite	0.5-40 nm (high absorption for all)	$10^5$ :1 (if same as visible)	$1/e$ loss after 40 nm thickness	Minimally	Calculations in this paper
Multilayer	30.4	16:1 max, 9:1 over 20° range	25	Yes, & is $\lambda$ dependent	Dhez, 1987
Multilayer	10-15	19:1	5-30	No	Maehara <i>et al</i> (1991)

Despite their changing the direction of the output beam, multilayer polarizers perform better than any other polarizer investigated in this work or known to the author at this time. Until a low loss and strongly birefringent material is found to work in the EUV, only visible and infrared applications will benefit from the high extinction ratio that prism-polarizers offer. Wire grid polarizers have the highest potential for use in the EUV, as advances in lithography make feasible grating periods approaching EUV wavelengths.

## References

- D. Attwood, *Soft X-Rays and Extreme Ultraviolet Radiation*, (Cambridge University Press, 1999).
- J.P. Auton, "Infrared Transmission Polarizers by Photolithography," *Applied Optics*, 6, 6 (1967).
- H.E. Bennett and J.M. Bennett, "Polarization," in *Handbook of Optics*, W.G. Driscoll and W. Vaughn, Eds. (McGraw-Hill, New York, 1978).
- G. R. Bird and M. Parrish, Jr., "The Wire Grid as a Near-Infrared Polarizer," *JOSA* 50, 886 (1960).
- S.P. Collins, "Polaroid H-Sheet as a polarizer for 33 keV X-rays," *Nuclear Instruments and Methods in Physics Research B*, 129, 289 (1997).
- P. Dhez, "Polarizers and Polarimeters in the X-UV Range," *Nuclear Instruments and Methods in Physics Research A* 261, 66 (1987).
- J. A. Dobrowolski and A. Waldorf, "High-performance thin film polarizer for the UV and visible spectral regions," *Applied Optics*, 20, 1, 111 (1981).
- T. K. Gaylord, E.N. Glytsis, and M. G. Moharam, *Applied Optics*, 26, 3123 (1987).
- M. Gruntman, Extreme-ultraviolet radiation filtering by freestanding transmission gratings, *Applied Optics*, 34, 5732 (1995).
- Eric Gullikson, X-Ray Interactions with Matter, [http://cindy.lbl.gov/optical\\_constants/getdb2.html](http://cindy.lbl.gov/optical_constants/getdb2.html) (2001).
- R. Winn Hardin, "Optical lithography gets nod from microchip industry", *SPIE OE Reports*, February 1999, <http://www.spie.org/web/oer/february/feb99/cover.html>.
- J. J. Huta and H. M. van Driel, "Coupled-wave analysis of lamellar metal transmission gratings for the visible and infrared," *J. Opt. Soc. Am. A*, 12 1118 (1995).
- Maehara, *et al*, Performance of a wideband soft-x-ray polarizer, *Applied Optics* 30 5018 (1991).
- N. Marcuvitz, *Waveguide Handbook*, M.I.T. Rad. Lab. Ser. (McGraw-Hill, New York, 1951).
- M. M. Murnane, H. C. Kapteyn, et al, "Efficient coupling of high intensity subpicosecond laser pulses into solids," *Applied Physics Letters*, 62, 1068 (1993).
- C.R. Nave, <http://hyperphysics.phy-astr.gsu.edu/hbase/phyopt/cdopt.html> (2000).
- J.R. Reitz, F. J. Milford, and R.W. Christy, *Foundations of Electromagnetic Theory*, (Addison-Wesley, Menlo Park, CA, 1993).
- M.L. Schattenburg, E.H. Anderson, H. Smith, "X-ray/VUV Transmission Gratings for Astrophysical and Laboratory Applications," *Physica Scripta*, 41, 13 (1997).